Title	What lies beneath? Reconstructing the primitive magmas fueling voluminous silicic volcanism using olivine-hosted melt inclusions
Author(s)	Barker, Simon J.; Rowe, Michael C.; Wilson, Colin J. N.; Gamble, John A.; Rooyakkers, Shane M.; Wysoczanski, Richard J.; Illsley-Kemp, Finnigan; Kenworthy, Charles C.
Publication date	2020-02-27
Original citation	Barker, S. J., Rowe, M. C., Wilson, C. J. N., Gamble, J. A., Rooyakkers, S. M., Wysoczanski, R. J., Illsley-Kemp, F. and Kenworthy, C. C. (2020) 'What lies beneath? Reconstructing the primitive magmas fueling voluminous silicic volcanism using olivine-hosted melt inclusions', Geology, 48, doi: 10.1130/G47422.1
Type of publication	Article (peer-reviewed)
Link to publisher's version	https://pubs.geoscienceworld.org/gsa/geology/article/doi/10.1130/G47422.1/582810/What-lies-beneath-Reconstructing-the-primitive http://dx.doi.org/10.1130/G47422.1 Access to the full text of the published version may require a subscription.
Rights	**© 2020 The Authors. Gold Open Access: This paper is published under the terms of the CC-BY license.** https://creativecommons.org/licenses/by/4.0/
Item downloaded from	http://hdl.handle.net/10468/9718

GEOLOGY | THE GEOLOGICAL SOCIETY OF AMERICA®

https://doi.org/10.1130/G47422.1

Manuscript received 22 July 2019
Revised manuscript received 21 January 2020
Manuscript accepted 23 January 2020

What lies beneath? Reconstructing the primitive magmas fueling voluminous silicic volcanism using olivine-hosted melt inclusions

Simon J. Barker[1]*, Michael C. Rowe[2], Colin J.N. Wilson[1], John A. Gamble[1,3], Shane M. Rooyakkers[1,4], Richard J. Wysoczanski[5], Finnigan Illsley-Kemp[1] and Charles C. Kenworthy[2]

[1]School of Geography, Environment and Earth Sciences, Victoria University of Wellington, P.O. Box 600, Wellington 6140, New Zealand
[2]School of Environment, University of Auckland, Private Bag 92019, Auckland 1142, New Zealand
[3]School of Biological, Earth and Environmental Sciences, University College Cork, Cork T12 YN60, Ireland
[4]Department of Earth and Planetary Sciences, McGill University, Montreal, Quebec H3A 0E8, Canada
[5]National Institute of Water and Atmospheric Research (NIWA), Private Bag 14901, Kilbirnie, Wellington 6021, New Zealand

ABSTRACT

Understanding the origins of the mantle melts that drive voluminous silicic volcanism is challenging because primitive magmas are generally trapped at depth. The central Taupō Volcanic Zone (TVZ; New Zealand) hosts an extraordinarily productive region of rhyolitic caldera volcanism. Accompanying and interspersed with the rhyolitic products, there are traces of basalt to andesite preserved as enclaves or pyroclasts in caldera eruption products and occurring as small monogenetic eruptive centers between calderas. These mafic materials contain MgO-rich olivines (Fo_{79-86}) that host melt inclusions capturing the most primitive basaltic melts fueling the central TVZ. Olivine-hosted melt inclusion compositions associated with the caldera volcanoes (intracaldera samples) contrast with those from the nearby, mafic intercaldera monogenetic centers. Intracaldera melt inclusions from the modern caldera volcanoes of Taupō and Okataina have lower abundances of incompatible elements, reflecting distinct mantle melts. There is a direct link showing that caldera-related silicic volcanism is fueled by basaltic magmas that have resulted from higher degrees of partial melting of a more depleted mantle source, along with distinct subduction signatures. The locations and vigor of Taupō and Okataina are fundamentally related to the degree of melting and flux of basalt from the mantle, and intercaldera mafic eruptive products are thus not representative of the feeder magmas for the caldera volcanoes. Inherited olivines and their melt inclusions provide a unique "window" into the mantle dynamics that drive the active TVZ silicic magmatic systems and may present a useful approach at other volcanoes that show evidence for mafic recharge.

INTRODUCTION

The magmatic systems that underpin large-scale silicic volcanism encompass large portions of the crust, with partially molten mushy reservoirs that can be thousands of cubic kilometers in volume (Bachmann and Huber, 2016). Although dominated by evolved compositions at upper-crustal levels, these systems are fundamentally driven from below by mantle-derived basaltic magmas. Therefore, the question arises: Are the basalts parental to the generation of large silicic volcanic eruptions derived from a different source compared to surrounding regional volcanism, or do they just represent locally enhanced (spatially and temporally) magma fluxes? This question is challenging to address because ascending primitive magmas are generally intercepted by large silicic reservoirs and are rarely erupted in unmodified form (Wiebe, 1994). Most evidence for mafic-silicic magma interactions therefore comes from mingled magmas, foreign crystal populations or zoned crystals, or co-erupted mafic enclaves (Bacon, 1986; Pritchard et al., 2013; Barker et al., 2016).

The central Taupō Volcanic Zone (TVZ; Fig. 1), New Zealand, is a frequently active and exceptionally productive region of Quaternary silicic volcanism, ultimately fueled by a basalt flux from the mantle that is unusually high for its continental arc setting (Wilson et al., 2009). The mantle processes driving this extreme flux are challenging to study because unmodified mantle-derived basalts are rarely erupted through the crustal silicic reservoirs. Over the past ~60 k.y., a volume of >780 km^3 magma (>99% silicic) has erupted from the central TVZ, almost entirely from two caldera volcanoes: Okataina and Taupō (Fig. 1; Wilson et al., 2009). Between Taupō and Okataina, volcanic activity since ca. 200 ka also includes scattered intercaldera mafic (basaltic to basaltic andesite), small-volume (collectively ~1 km^3) eruptive centers that are typically aligned along northeast-southwest–trending faults (Gamble et al., 1993; Table DR1 in the GSA Data Repository[1]).

Here, we investigated the compositions of primitive melts feeding young volcanism in the central TVZ to see if there were any differences between the caldera centers and the less active areas in between. We used the novel approach of analyzing olivine-hosted melt inclusions (MIs) contained within juvenile mafic materials that

---

*E-mail: simon.barker@vuw.ac.nz

[1]GSA Data Repository item 2020145, geochemical data tables, primary melt–corrected trace-element figure, and trace-element models, is available online at http://www.geosociety.org/datarepository/2020/, or on request from editing@geosociety.org.

CITATION: Barker, S.J., et al., 2020, What lies beneath? Reconstructing the primitive magmas fueling voluminous silicic volcanism using olivine-hosted melt inclusions: Geology, v. 48, p. , https://doi.org/10.1130/G47422.1

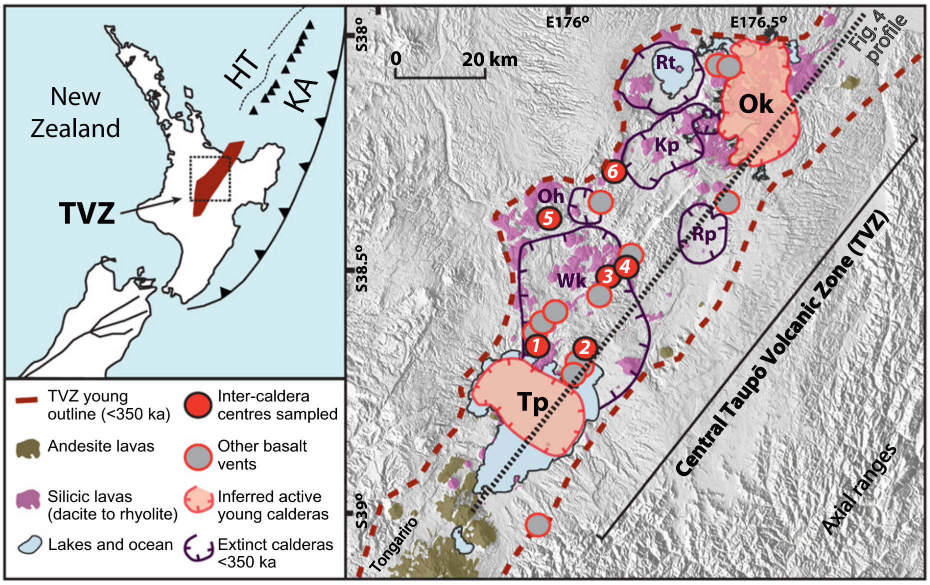

Figure 1. Map showing setting of Taupō Volcanic Zone (TVZ) in New Zealand (inset) with sample locations. Outlines of calderas and young TVZ (≤350 ka) boundary are from Wilson et al. (2009), and locations and compositions of young lavas are from Leonard et al. (2010). Location of Kermadec arc (KA) northeast of New Zealand is shown by black triangles, and Havre Trough (HT) back-arc basin is denoted by black dashed line. Intercaldera samples discussed here: 1—Kinloch, 2—Punatekahi, 3—Tatua, 4—Kakuki, 5—Ongaroto, 6—Harry Johnson Road. The two most recently active caldera volcanoes Tp (Taupō) and Ok (Okataina) are sources for intracaldera samples discussed here. Other caldera outlines: Kp—Kapenga, Oh—Ohakuri, Rp—Reporoa, Rt—Rotorua, and Wk—Whakamaru. See Table DR3 (see footnote 1) for further sampling details. Black dashed line shows approximate line of schematic cross section in Figure 4.

were erupted during rhyolitic events at the caldera volcanoes and compared these with their counterparts from the interspersed intercaldera mafic centers (Fig. 2A; Fig. DR2).

OLIVINE IN CENTRAL TVZ ERUPTIVE PRODUCTS

We studied olivine crystals from mafic enclaves in deposits of the 25.5 ka Oruanui and 3.5 ka Waimihia eruptions from Taupō, and the 1314 Kaharoa eruption from Okataina (Fig. 2A; Fig. DR2). The enclaves are interpreted as juvenile because they have crenulated chilled margins and adhering rhyolitic glass, and they host rhyolite-derived crystals ingested during syneruptive interactions (Leonard et al., 2002; Rooyakkers et al., 2018). Olivines in these enclaves are Mg-rich (Fo_{80-86}) [Fo = molar Mg/(Mg + Fe^{2+}) × 100] and commonly contain MIs that are mostly <20 μm, but sometimes up to 100 μm, across (Fig. 2B; Table DR3). The MIs are variably crystalline due to residence in the rhyolitic magmas, which promoted crystal growth from the inclusion wall (e.g., Danyushevsky et al., 2000). Two basaltic scoria units from Okataina were sampled for comparison with the 1886 Tarawera and 21.9 ka Okareka eruption products containing rare olivines (Fo_{79-82}; Table DR3). For contrast, we sampled olivines from six small-volume mafic centers between Taupō and Okataina (Fig. 1), the products of which represent the most primitive compositions to reach the surface in this area over the past ~200 k.y. (Gamble et al., 1993; Table DR1). Olivines in the sampled units overlap in composition (Fo_{78-90}) with the caldera-related olivines (Table DR3), but their MIs are less common and tend to be smaller, and all have experienced some postentrapment crystallization.

MIs were homogenized through standard 1 atm heating experiments to remove postentrapment crystallization (Danyushevsky et al., 2002; Rowe et al., 2015). Rehomogenized MIs and olivine hosts were analyzed for major elements by electron microprobe (Table DR3), and then MIs >35 μm across were analyzed for trace-element concentrations by laser-ablation inductively coupled plasma–mass spectrometry (Table DR4). Following analysis, measured glass compositions were corrected for over/underheating (Rowe et al., 2015) and olivine-melt postentrapment reequilibration (Fe loss) using Petrolog3 (Danyushevsky and Plechov, 2011). A fundamental assumption required for Fe-loss corrections is that the whole-rock Fe content is representative of the MIs prior to entrapment. While a good approximation for basaltic lava, all enclaves showed clear macroscopic evidence for mixing with the silicic magma (Fig. 2A). In these instances, Fe contents of MIs closest to equilibrium with their host olivine with Fe-Mg distribution coefficients (K_D) of ~0.3 were used as the corrected Fe values (Rowe et al., 2011; full analytical details in Table DR3).

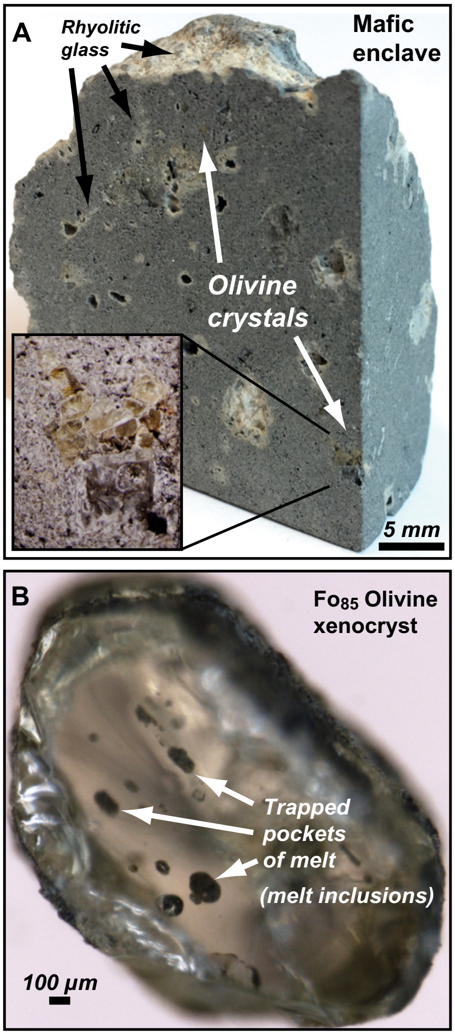

Figure 2. Images of representative mafic samples from Taupō volcano (New Zealand) highlighting the context of materials analyzed in this study. (A) Juvenile mafic enclave from the 25.4 ka Oruanui eruption (P560) hosting sampled olivine crystals (photo inset). Note the crenulated margin to the enclave and adhering and ingested rhyolitic pumiceous glass, taken to indicate the molten nature of the enclave upon entrainment (e.g., Rooyakkers et al., 2018). (B) High-Fo olivine hosting multiple large, but partially crystalline, melt inclusions. See Figure DR2 (see footnote 1) for more images and Table DR3 for details of melt inclusion rehomogenization and analytical techniques.

COMPOSITION OF CENTRAL TVZ OLIVINE-HOSTED MELT INCLUSIONS

MIs in olivines derived from the five caldera-related units (intracaldera samples) were among the most primitive melt compositions identified from the TVZ to date, forming a distinct compositional group with low TiO_2, P_2O_5, and Na_2O contents when compared to MIs from the intercaldera centers (Figs. 3A and 3B). Compositional differences between MIs from the two Taupō samples were minor, with Oruanui MIs having slightly lower TiO_2 and Na_2O contents

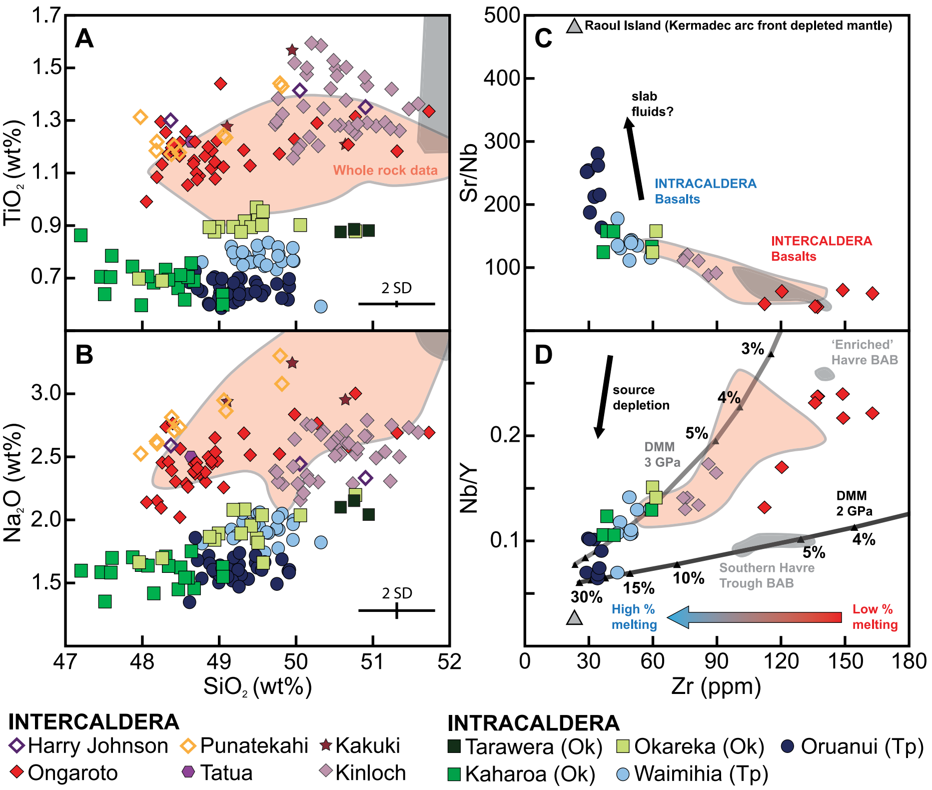

Figure 3. Selected geochemical data from homogenized olivine-hosted melt inclusions (MIs) from intra- and intercaldera mafic eruptive products from the central Taupō Volcanic Zone (TVZ, New Zealand). (A) TiO_2 versus SiO_2. (B) Na_2O versus SiO_2. (C) Sr/Nb (measure of subduction-related fluid component) versus Zr (measure of degree of partial melting or depletion). (D) Nb/Y (degree of mantle depletion) versus Zr. All data have been corrected for crystallization and olivine-melt postentrapment reequilibration; 2 standard deviation (SD) errors are shown by the black cross, and were calculated from repeated analysis of secondary standards (not shown for trace elements because they were typically smaller than the size of the symbols; see Tables DR3 and DR4 [see footnote 1] for further details). Red field represents whole-rock X-ray fluorescence data from host intercaldera basalts sampled in this study (Table DR1) and data from Gamble et al. (1993), Rooney and Deering (2014), and Waight et al. (2017) for comparison; gray field represents pillow glass compositions from Havre Trough back-arc basalt (BAB) lavas from Wysoczanski et al. (2006). Data from Raoul Island (Kermadec arc) basalt (gray triangle) are from Barker et al. (2013). For intracaldera MIs: Ok—Okataina, Tp—Taupō. Trace-element models for partial melting are shown for nonfractional batch melting adopting a deep (3 GPa) garnet-bearing source (light gray) or a shallow (2 GPa) source (dark gray) of depleted mid-oceanic ridge basalt (MORB) mantle (DMM), from Salters and Strake (2004). Modal mineralogies of deep and shallow mantle sources, and partition coefficients used in batch melting calculations are those recommended by Salters and Strake (2004, and references therein). Black triangles represent 1% increments up to 5% melting, and then 5% increments up to 30% melting.

than those from Waimihia. Okareka MIs from Okataina showed slightly higher TiO_2 than the other intracaldera samples, but otherwise Okataina and Taupō MIs were very similar in major-element compositions. Major-element compositions of MIs from the six intercaldera centers overlapped with published whole-rock data for monogenetic centers throughout the TVZ (red field in Fig. 3).

Trace-element data further highlighted contrasts between the intra- and intercaldera samples. MIs from Taupō and Okataina showed low abundances of incompatible trace elements (e.g., Zr = 30–60 ppm, Nb = 1–3 ppm, and Y = 10–19 ppm) and rare earth elements (Figs. 3C and 3D; Table DR4). Incompatible element concentrations were lowest in the Oruanui-derived MIs, which also had higher Sr/Nb and Th/Nb ratios than all other examples. In comparison, MIs from one of the intercaldera samples (Ongaroto) showed the highest concentrations of Zr (112–163 ppm), Nb (4–7 ppm), and Y (27–33 ppm). Incompatible trace-element concentrations in MIs from another intercaldera sample (Kinloch) fell between those of Ongaroto and the intracaldera values, overlapping with published whole-rock trace-element data from other intercaldera basalts from the TVZ (red field in Figs. 3C and 3D).

DISCUSSION

Reconstructing the Primitive Melt Compositions

In general, the geochemical characteristics of mafic to intermediate arc magmas inevitably reflect variable degrees of crustal hybridization and differentiation, masking the primary magma compositions (Waight et al., 2017). Although we targeted MIs in the most primitive olivines, these crystals still recorded variable forsterite and NiO contents (Table DR3), consistent with varying degrees of crystallization at the time of melt entrapment. We therefore back-calculated olivine-hosted MI compositions to a primary mantle–derived magma composition using the PRIMACALC2 software (Kimura and Ariskin, 2014). Most of the MIs experienced only olivine fractionation (typically <20%), but some from Waimihia and Kinloch also experienced some clinopyroxene fractionation (Table DR5). Trace-element abundances, back-calculated using stepwise addition of the fractionated minerals, demonstrated, however, that compositional differences between the intra- and intercaldera MIs reflect actual differences in primary melt compositions and not just differentiation processes (Fig. DR6).

Compositional Contrasts Between Intra- and Intercaldera Melts

Despite the relatively small geographic distances involved (Fig. 1), there are major differences in the melt compositions entering the crust beneath Taupō and Okataina volcanoes versus those represented in the intercaldera centers. Intracaldera olivine-hosted MIs associated with silicic eruptions have lower high field strength element (HFSE) concentrations, which reflect fundamental differences in the mantle melting regimes beneath versus between the caldera volcanoes in the central TVZ. Compositions from the intracaldera MIs can be modeled by ~10%–30% melting of a depleted mid-ocean-ridge mantle (DMM) source across a range of different pressures and mineralogies (Figs. 3C and 3D; Table DR4). Such compositions could reflect mantle source depletion through previous melt extraction, although MIs from the largest eruption considered (Oruanui) reflect the highest percentage of source melting (~20%–30%) with a stronger subduction signature, suggesting that melting may be directly linked to enhanced fluid fluxes from the slab (e.g., flux melting; Fig. 3C; Rowe et al., 2009). In contrast, the intercaldera MI (and their host rock) compositions can be modeled by 3%–10% partial melting of DMM. Alternatively, the subarc mantle beneath the TVZ may be heterogeneous (e.g., Waight et al., 2017) and enriched for the intercaldera basalts. Intercaldera TVZ basalts have higher HFSE concentrations, with trace-element compositions that extend to those observed in primitive lavas erupted in the Havre Trough back-arc basin, offshore to the north of New Zealand (Figs. 1 and 3). There, magmatism is primarily driven by low-degree decompression melting with variable, but lesser, inputs from slab fluids, reflected in low Sr/Nb, Ba/Nb, and Th/Nb values (Wysoczanski et al., 2006). The central TVZ is a segment of rifted continental arc with extension rates of ~8–15 mm/yr^{-1}, similar to those in the Havre Trough, which averages ~20 mm/yr^{-1} (Hamling et al., 2015; Caratori Tontini et al., 2019). Rift-associated decompression melting is therefore inferred to play a major role in central TVZ magmatism.

Implications for Central TVZ Magmatism

The central TVZ is a complex rifting arc (Fig. 1), making it challenging to explain temporal and spatial changes in volcanism. Compositional contrasts between olivine-hosted MIs from intercaldera centers versus intracaldera eruptive products show that the basaltic feedstocks entering the central TVZ crust reflect both lower degrees of more decompression-driven melting (intercaldera examples) and higher degrees of more subduction-related flux melting (intracaldera examples). These findings highlight two important aspects of modern silicic volcanism in the central TVZ. First, there is a fundamental mantle control on the locations and productivities of Taupō and Okataina, driven by higher degrees of mantle melting and supply rates of primitive magmas into the crust (Fig. 4). This is supported by seismic imaging of the mantle wedge beneath the TVZ, which shows that there are large spatial variations in mantle melting, consistent with variable fluid flux from the subducting slab (Eberhart-Phillips et al., 2020). Mantle melting beneath the TVZ calderas may therefore reflect a combination of both rift-induced decompression melting and enhanced fluid-induced flux melting. Thermal calculations of magma input to the crust modeled using both volcanic and geothermal outputs indicate that the relative degrees of partial melting broadly match the relative rates of mafic magma supply, whereby 4–10 times more mafic melt per unit length of arc is focused into the crust beneath the caldera volcanoes, which ultimately provides the magma flux required to sustain and drive such large-scale silicic reservoirs (Fig. 4; Table DR7). In contrast, measurements of crustal seismic anisotropy suggest that geothermal activity in the area between Taupō and Okataina is driven by lower-crustal magmatism, and that shallow magma reservoirs of a comparable size do not exist in this region (Illsley-Kemp et al., 2019). Pervasive normal faulting in the area between Okataina and Taupō may also help the small-degree basaltic melts to erupt (Leonard et al., 2010). Second, the compositional contrasts between the two data suites imply that compositions of mafic magmas feeding caldera systems are distinctly different than those of peripheral mafic centers, even over distances of <10–20 km. Compositions of the monogenetic intercaldera basalts should thus not be used to infer the mantle melting conditions for caldera-related silicic volcanism in the central TVZ (cf. Rooney and Deering, 2014). A complicating factor is that the foci of silicic volcanism have shifted through time, with multiple caldera centers active at different times and locations in the central TVZ (Fig. 1; Gravley et al., 2016). This history would suggest that the degrees of mantle melting and/or delivery pathways of melt to the base of the crust have changed through time.

Inherited Olivines Provide a Geochemical Window through the Crust

Despite occurring only in trace amounts, inherited olivines and their MI cargoes provide unique insights into the subcrustal melt compositions that ultimately have given rise to large-scale, caldera-related silicic volcanism in the central TVZ. We took advantage of two factors in this study: (1) the entrapment and preservation of the most primitive melts in early crystallized high-Fo olivines, and (2) the survival of these olivines into the crustally evolved and contaminated enclaves in silicic eruptions or in basaltic magmas that ascended rapidly. Targeting high-Mg olivines in the trace mafic "contaminants" of silicic deposits thus provides a new way to see through the crustal overprints in silicic magmatic systems in general, not just in the extreme example in the central TVZ. Our approach is applicable to any magmatic system where mafic enclaves have been documented, and it offers new possibilities to investigate the dynamics of silicic magmatic systems associated with caldera-forming events.

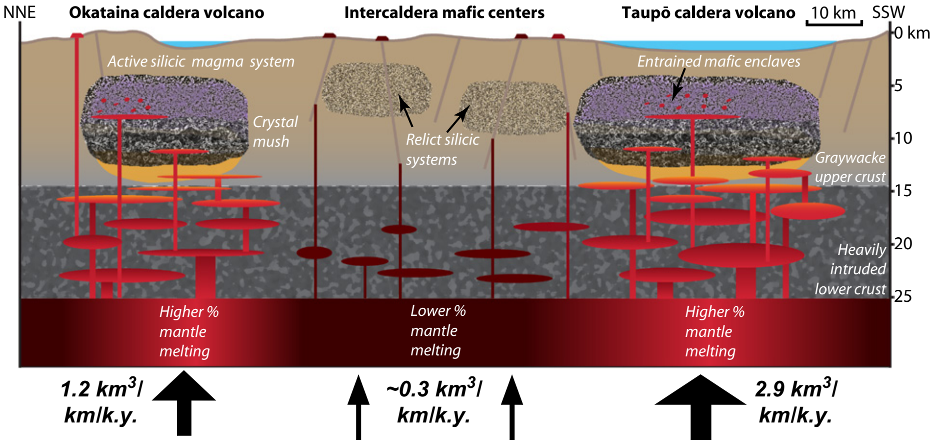

Figure 4. Scaled cross section of crust and upper mantle beneath the central Taupō Volcanic Zone (TVZ, New Zealand), along the line marked in Figure 1, highlighting the contrasts in mantle-melt inputs and crustal pathways to the surface between caldera volcanoes and the intervening sector of the central TVZ. Relict silicic magma systems (active from 350 to 250 ka) refer to those from Gravley et al. (2016). Magma fluxes across the central TVZ were calculated by considering total heat output from geothermal systems (Bibby et al., 1995) and total eruptive volumes over the past ~60 k.y. (Wilson et al., 2009), assuming that 1 unit volume of rhyolite requires 5× that volume of basalt (see details in Table DR7 [see footnote 1]).

ACKNOWLEDGMENTS

We thank Adam Kent, Tyrone Rooney, Roger Nielsen, and James Muirhead for helpful discussions, and Joel Baker for input during the early stages of this research. Frank Tepley, Melissa Drignon, Bruce Charlier, and Stuart Morrow are thanked for analytical assistance. We thank Esteban Gazel, Audrey Bouvier, Maxim Portnyagin, Florence Bégué, and two anonymous reviewers for their helpful comments and suggestions, and James Schmitt for editorial handling. We acknowledge the Marsden Fund of the Royal Society of New Zealand (grant VUW1627) awarded to Barker and ongoing support from the ECLIPSE project (contract RTVU1704) funded by the New Zealand Ministry of Business, Innovation and Employment.

REFERENCES CITED

Bachmann, O., and Huber, C., 2016, Silicic magma reservoirs in Earth's crust: The American Mineralogist, v. 101, p. 2377–2404, https://doi.org/10.2138/am-2016-5675.

Bacon, C.R., 1986, Magmatic inclusions in silicic and intermediate volcanic rocks: Journal of Geophysical Research, v. 91, p. 6091–6112, https://doi.org/10.1029/JB091iB06p06091.

Barker, S.J., Wilson, C.J.N., Baker, J.A., Millet, M.-A., Rotella, M.D., Wright, I.C., and Wysoczanski, R.J., 2013, Geochemistry and petrogenesis of silicic magmas in the intra-oceanic Kermadec arc: Journal of Petrology, v. 54, p. 351–391, https://doi.org/10.1093/petrology/egs071.

Barker, S.J., Wilson, C.J.N., Morgan, D.J., and Rowland, J.V., 2016, Rapid priming, accumulation and recharge of magma driving recent eruptions at a hyperactive caldera volcano: Geology, v. 44, p. 323–326, https://doi.org/10.1130/G37382.1.

Bibby, H.M., Caldwell, T.G., Davey, F.J., and Webb, T.H., 1995, Geophysical evidence on the structure of the Taupo Volcanic Zone and its hydrothermal circulation: Journal of Volcanology and Geothermal Research, v. 68, p. 29–58, https://doi.org/10.1016/0377-0273(95)00007-H.

Caratori Tontini, F., Bassett, D., de Ronde, C.E., Timm, C., and Wysoczanski, R., 2019, Early evolution of a young back-arc basin in the Havre Trough: Nature Geoscience, v. 12, p. 856–862, https://doi.org/10.1038/s41561-019-0439-y.

Danyushevsky, L.V., and Plechov, P., 2011, Petrolog3: Integrated software for modeling crystallization processes: Geochemistry Geophysics Geosystems, v. 12, Q07021, https://doi.org/10.1029/2011GC003516.

Danyushevsky, L.V., Della-Pasqua, F.N., and Sokolov, S., 2000, Re-equilibration of melt inclusions trapped by magnesian olivine phenocrysts from subduction-related magmas: Petrological implications: Contributions to Mineralogy and Petrology, v. 138, p. 68–83, https://doi.org/10.1007/PL00007664.

Danyushevsky, L.V., McNeill, A.W., and Sobolev, A.V., 2002, Experimental and petrological studies of melt inclusions in phenocrysts from mantle-derived magmas: An overview of techniques, advantages and complications: Chemical Geology, v. 183, p. 5–24, https://doi.org/10.1016/S0009-2541(01)00369-2.

Eberhart-Phillips, D., Bannister, S., and Reyners, M., 2020, Attenuation in the mantle wedge beneath super-volcanoes of the Taupo Volcanic Zone, New Zealand: Geophysical Journal International, v. 220, p. 703–723, https://doi.org/10.1093/gji/ggz455.

Gamble, J.A., Smith, I.E.M., McCulloch, M.T., Graham, I.J., and Kokelaar, B.P., 1993, The geochemistry and petrogenesis of basalts from the Taupo Volcanic Zone and Kermadec Island Arc, S.W. Pacific: Journal of Volcanology and Geothermal Research, v. 54, p. 265–290, https://doi.org/10.1016/0377-0273(93)90067-2.

Gravley, D.M., Deering, C.D., Leonard, G.S., and Rowland, J.V., 2016, Ignimbrite flare-ups and their drivers: A New Zealand perspective: Earth-Science Reviews, v. 162, p. 65–82, https://doi.org/10.1016/j.earscirev.2016.09.007.

Hamling, I.J., Hreinsdóttir, S., and Fournier, N., 2015, The ups and downs of the TVZ: Geodetic observations of deformation around the Taupo Volcanic Zone, New Zealand: Journal of Geophysical Research–Solid Earth, v. 120, p. 4667–4679, https://doi.org/10.1002/2015JB012125.

Illsley-Kemp, F., Savage, M.K., Wilson, C.J.N., and Bannister, S., 2019, Mapping stress and structure from subducting slab to magmatic rift: Crustal seismic anisotropy of the North Island, New Zealand: Geochemistry Geophysics Geosystems, v. 20, p. 5038–5056, https://doi.org/10.1029/2019GC008529.

Kimura, J.-I., and Ariskin, A.A., 2014, Calculation of water-bearing primary basalt and estimation of source mantle conditions beneath arcs: PRIMACALC2 model for WINDOWS: Geochemistry Geophysics Geosystems, v. 15, p. 1494–1514, https://doi.org/10.1002/2014GC005329.

Leonard, G.S., Cole, J.W., Nairn, I.A., and Self, S., 2002, Basalt triggering of the c. A.D. 1305 Kaharoa rhyolite eruption, Tarawera Volcanic Complex, New Zealand: Journal of Volcanology and Geothermal Research, v. 115, p. 461–486, https://doi.org/10.1016/S0377-0273(01)00326-2.

Leonard, G.S., Begg, J.G., and Wilson, C.J.N., compilers, 2010, Geology of the Rotorua Area: Lower Hutt, New Zealand, GNS Science, Institute of Geological & Nuclear Sciences Geological Map 5, scale 1:250,000.

Pritchard, C.J., Larson, P.B., Spell, T.L., and Tarbert, K.D., 2013, Eruption-triggered mixing of extra-caldera basalt and rhyolite complexes along the East Gallatin–Washburn fault zone, Yellowstone National Park, WY, USA: Lithos, v. 175–176, p. 163–177, https://doi.org/10.1016/j.lithos.2013.04.022.

Rooney, T.O., and Deering, C.D., 2014, Conditions of melt generation beneath the Taupo Volcanic Zone: The influence of heterogeneous mantle inputs on large-volume silicic systems: Geology, v. 42, p. 3–6, https://doi.org/10.1130/G34868.1.

Rooyakkers, S.M., Wilson, C.J.N., Schipper, C.I., Barker, S.J., and Allan, A.S.R., 2018, Textural and micro-analytical insights into mafic-felsic interactions during the Oruanui eruption, Taupo: Contributions to Mineralogy and Petrology, v. 173, p. 35, https://doi.org/10.1007/s00410-018-1461-6.

Rowe, M.C., Kent, A.J.R., and Nielsen, R.L., 2009, Subduction influence on oxygen fugacity and trace and volatile elements in basalts across the Cascade volcanic arc: Journal of Petrology, v. 50, p. 61–91, https://doi.org/10.1093/petrology/egn072.

Rowe, M.C., Peate, D.W., and Newbrough, A., 2011, Compositional and thermal evolution of olivine-hosted melt inclusions in small-volume basaltic eruptions: A “simple” example from Dotsero Volcano, NW Colorado: Contributions to Mineralogy and Petrology, v. 161, p. 197–211, https://doi.org/10.1007/s00410-010-0526-y.

Rowe, M.C., Lassiter, J.C., and Goff, K., 2015, Basalt volatile fluctuations during continental rifting: An example from the Rio Grande Rift, USA: Geochemistry Geophysics Geosystems, v. 16, p. 1254–1273, https://doi.org/10.1002/2014GC005649.

Salters, V.J.M., and Strake, A., 2004, Composition of the depleted mantle: Geochemistry Geophysics Geosystems, v. 5, Q05004, https://doi.org/10.1029/2003GC000597.

Waight, T.E., Troll, V.R., Gamble, J.A., Price, R.C., and Chadwick, J.P., 2017, Hf isotope evidence for variable slab input and crustal addition in basalts and andesites of the Taupo Volcanic Zone, New Zealand: Lithos, v. 284–285, p. 222–236, https://doi.org/10.1016/j.lithos.2017.04.009.

Wiebe, R.A., 1994, Silicic magma chambers as traps for basaltic magmas: The Cadillac Mountain intrusive complex, Mount Desert Island, Maine: The Journal of Geology, v. 102, p. 423–437, https://doi.org/10.1086/629684.

Wilson, C.J.N., Gravley, D.M., Leonard, G.S., and Rowland, J.V., 2009, Volcanism in the central Taupo Volcanic Zone, New Zealand: Tempo, styles and controls, *in* Thordarson, T., et al., eds., Studies in Volcanology: The Legacy of George Walker: International Association of Volcanology and Chemistry of the Earth’s Interior Special Publication 2, p. 225–247, https://doi.org/10.1144/IAVCEI002.12.

Wysoczanski, R.J., Wright, I.C., Gamble, J.A., Hauri, E.H., Luhr, J.F., Eggins, S.M., and Handler, M.R., 2006, Volatile contents of Kermadec arc–Havre Trough pillow glasses: Fingerprinting slab-derived aqueous fluids in the mantle sources of arc and back-arc lavas: Journal of Volcanology and Geothermal Research, v. 152, p. 51–73, https://doi.org/10.1016/j.jvolgeores.2005.04.021.

Printed in USA